CO2-induced shift in microbial activity affects carbon trapping and water quality in anoxic bioreactors

Matthew F. Kirk, Eugenio F. U. Santillan, Robert A. Sanford, Susan J. Altman

Published Version Information

Citation: Kirk, M. F., Santillan, E. F. U., Sanford, R. A., & Altman, S. J. (2013). CO2-induced shift in microbial activity affects carbon trapping and water quality in anoxic bioreactors. Geochimica et Cosmochimica Acta, 122, 198-208.

Digital Object Identifier (DOI): doi:10.1016/j.gca.2013.08.018

Publisher's Link: http://www.sciencedirect.com/science/article/pii/S0016703713004626

CO_2-Induced Shift in Microbial Activity Affects Carbon Trapping and Water Quality in Anoxic Bioreactors

Matthew F. Kirk[1,4,*], Eugenio F. U. Santillan[2], Robert A. Sanford[3], Susan J. Altman[1]

[1]Geochemistry Department, Sandia National Laboratories, P.O. Box 5800, Albuquerque, NM 87185-0754, USA

[2]Jackson School of Geosciences, University of Texas at Austin, 1 University Station C9000, Austin, TX 78712-0254, USA

[3]Department of Geology, University of Illinois, 1301 W. Green St. Urbana, IL 61801, USA

[4]Current address: Department of Geology, Kansas State University, Manhattan, KS 66506-3201, USA

*Corresponding author: matthew.f.kirk@gmail.com, +1 785-532-6724 (office), +1 785-532-5159 (fax)

Submitted to:

Geochimica et Cosmochimica Acta

Initially: March 29, 2013

In revised form: August 9, 2013

Abstract

Microbial activity is a potentially important yet poorly understood control on the fate and environmental impact of CO_2 that leaks into aquifers from deep storage reservoirs. In this study we examine how variation in CO_2 abundance affected competition between Fe(III) and SO_4^{2-}-reducers in anoxic bioreactors inoculated with a mixed-microbial community from a freshwater aquifer. We performed two sets of experiments: one with low CO_2 partial pressure (~0.02 atm) in the headspace of the reactors and one with high CO_2 partial pressure (~1 atm). A fluid residence time of 35 days was maintained in the reactors by replacing one-fifth of the aqueous volume with fresh medium every seven days. The aqueous medium was composed of groundwater amended with small amounts of acetate (250 μM), phosphate (1 μM), and ammonium (50 μM) to stimulate microbial activity. Synthetic goethite (1 mmol) and SO_4^{2-} (500 μM influent concentration) were also available in each reactor to serve as electron acceptors. Results of this study show that higher CO_2 abundance increased the ability of Fe(III) reducers to compete with SO_4^{2-} reducers, leading to significant shifts in CO_2 trapping and water quality. Mass-balance calculations and pyrosequencing results demonstrate that SO_4^{2-} reducers were dominant in reactors with low CO_2 content. They consumed 85% of the acetate after acetate consumption reached steady state while Fe(III) reducers consumed only 15% on average. In contrast, Fe(III) reducers were dominant during that same interval in reactors with high CO_2 content, consuming at least 90% of the acetate while SO_4^{2-} reducers consumed a negligible amount (<1%). The higher rate of Fe(III) reduction in the high-CO_2 bioreactors enhanced CO_2 solubility trapping relative to the low-CO_2 bioreactors by increasing alkalinity generation (6X). Hence, the shift in microbial activity we observed was a positive feedback on CO_2 trapping. More rapid Fe(III) reduction degraded water quality, however, by leading to high Fe(II) concentration.

Keywords: Geological carbon storage, CO_2 leakage, iron reduction, sulfate reduction, microbial reaction rates, groundwater, pyrosequencing

1. INTRODUCTION

Carbon capture and geological storage is one option in the range of actions that can be used to help stabilize atmospheric CO_2 levels despite anticipated increases in CO_2 production (IPCC, 2005). The process involves capturing CO_2 before it is released to the atmosphere and injecting it into a deep subsurface reservoir (Benson and Cole, 2008). CO_2 would be injected at depths >800 m where it would exist as a buoyant supercritical phase (IPCC, 2005). A low-permeability caprock overlying a storage reservoir is necessary to limit upward migration of supercritical CO_2. Over time, CO_2 would also be trapped by dissolution into water, formation of minerals, and capillary trapping (Benson and Cole, 2008).

Although this mitigation strategy is promising, leakage of CO_2 from storage reservoirs is a major environmental concern because the CO_2 can cause reactions that negatively impact water quality in overlying freshwater aquifers. The CO_2 could also eventually reach the atmosphere, undermining attempts to limit greenhouse gas accumulation. Potential leakage pathways include faults and fractures, abandoned wells, and diffusive leakage through caprocks (Celia and Nordbotten, 2009; IPCC, 2005). CO_2 can negatively affect water quality by lowering pH, causing minerals to dissolve, increasing solute levels, and mobilizing both organic and inorganic contaminants (Apps et al., 2010; Kharaka et al., 2010; Little and Jackson, 2010; Lu et al., 2010; Wang and Jaffe, 2004; Wilkin and Digiulio, 2010; Zheng et al., 2009).

Whereas several studies have examined how CO_2 leakage would react chemically with water and minerals in the subsurface, relatively little research has examined how CO_2 leakage would affect subsurface microbial processes (Harvey et al., 2013). Filling this knowledge gap is important because microorganisms can strongly influence the physical and chemical properties of

the subsurface. Microbes, for example, can lower the permeability of a porous medium by orders of magnitude (Gerlach and Cunningham, 2010), control the mobility of organic and inorganic contaminants (Lovley, 2001), and drive both mineral dissolution and precipitation (Benzerara et al., 2011; Uroz et al., 2009). As a result, the impact that an increase in CO_2 abundance has on subsurface microbial populations will affect the fate of that CO_2 and its impact on subsurface water resources.

Much of the research on microbial interactions with CO_2 has examined how CO_2 affects cell survival. High pressure CO_2 can kill cells by extracting intracellular materials, disabling enzymes, and causing the release of toxic trace elements from minerals (Bertoloni et al., 2006; Oule et al., 2006; Santillan et al., 2013; Wimmer and Zarevucka, 2010). Numerous studies have shown, however, that microorganisms are capable of colonizing environments with aqueous CO_2 concentrations that are high relative to most natural waters (e.g., Inagaki et al., 2006; Oppermann et al., 2010; Videmsek et al., 2009; Yakimov et al., 2002). Hence, microbial communities are capable of withstanding at least moderate increases in CO_2 abundance. Cells that have Gram positive cell walls, exist within biofilms, and produce spores appear to be better able to survive exposure to high levels of CO_2 (Mitchell et al., 2008; Zhang et al., 2006). Carbonate minerals can also promote cell survival by providing rapid pH buffering (Wu et al., 2010).

Although previous research shows that communities can persist following an increase in CO_2 abundance, it is unclear whether an increase in CO_2 could affect competition between different metabolic groups. In this study, we use bioreactor experiments with periodic fluid replacement to examine how an increase in CO_2 affects competition between Fe(III) and SO_4^{2-}-reducing microorganisms. Our objectives were to monitor the activity of each group and to assess how microbial activity impacted CO_2 trapping and water quality. We focus on these groups of microorganisms because thermodynamic relationships suggest that variation in CO_2 abundance would affect them differently. As pH decreases, the free energy yield of microbial Fe(III) reduction increases rapidly while that of microbial SO_4^{2-} reduction changes little (Bethke et al., 2011; Postma

and Jakobsen, 1996). A decrease in pH associated with increasing CO_2 abundance, therefore, could affect competition between these groups for electron donors (Kirk, 2011). Moreover, these groups of microorganisms are also widespread in subsurface environments (Bethke et al., 2011; Lovley and Chapelle, 1995). Hence, they are likely present in many of the aquifers that could be exposed to CO_2 leakage.

We performed two sets of experiments: one with a CO_2 partial pressure of about 0.02 atm in the headspace of the reactors and one with a CO_2 partial pressure of about 1 atm. Hereafter these experiments are referred to as the "low-CO_2" and the "high-CO_2" experiments, respectively. Comparison of the results between these sets of experiments provides a measure of the extent to which variation in CO_2 abundance influenced chemistry and microbial activity in our study.

2. MATERIALS AND METHODS

2.1. Inoculum

Microorganisms used in the bioreactors were collected during November 2011 from the Mahomet aquifer, a freshwater aquifer in central Illinois (Kempton et al., 1991). Note that microorganisms from the aquifer were not used in an attempt to simulate the aquifer experimentally but rather to seed the bioreactors with a mixed-community of microorganisms that naturally co-exist. The sample was collected as described previously by lowering a sterile bag of aquifer sediment into a well, CHM95A, and allowing it to incubate for 12 months (Flynn et al., 2008). Sediment removed from the bag after the incubation was immediately placed into an anaerobic culture tube (Belco Glass Inc.) completely filled with oxygen-free groundwater collected previously from the aquifer. The tube was then quickly plugged with a butyl-rubber stopper, sealed with an aluminum crimp, and stored for 5 months until use. To limit changes in community composition during storage, the sample was stored in the dark at 4°C. The extent to which cold storage affected the composition of the microbial community was not evaluated. However, because

122 the same sample was used to inoculate all of our reactors, any changes that occurred during storage
123 would have affected each set of experiments equally.
124 Well CHM95A was chosen for collection of an inoculum sample for this study because
125 previous research showed that Fe(III) and SO_4^{2-}-reducing microorganisms are active where the well
126 is completed (Flynn et al., 2012). In general, Fe(III) reducers are present throughout the Mahomet
127 aquifer, reflecting the widespread availability of Fe(III) oxyhydroxides, anoxic conditions, and
128 limited availability of nitrate (Flynn et al., 2013; Flynn et al., 2012; Kelly et al., 2005). In addition to
129 Fe(III) reducers, SO_4^{2-} reducers are active where SO_4^{2-} concentration exceeds about 0.03 mM and
130 methanogens, where SO_4^{2-} concentration falls below that level (Flynn et al., 2013; Flynn et al.,
131 2012). Groundwater from CHM95A contains about 0.14 mM SO_4^{2-} (Burch, 2008; Flynn et al., 2012),
132 consistent with previous detection of both Fe(III and SO_4^{2-} reducers there.
133

134 **2.2. Groundwater medium**

135 Groundwater from the Mahomet aquifer was used to make aqueous medium for the
136 experiment, helping to limit the extent to which culturing effects would have limited growth of cells.
137 The water was collected one year prior to the experiment from well CHM95D. The well produces
138 water with similar bulk composition to that from CHM95A, which is located about 27 km away
139 (Burch, 2008). Previous workers have found little nitrate (< 1 μM) in groundwater from the well
140 (Burch, 2008; Flynn et al., 2012). During storage at 4°C prior to the experiment, however, a small
141 concentration of nitrate had accumulated in the water presumably from ammonium oxidation. The
142 water initially contained about 57 μM ammonium. We removed the nitrate before the experiment
143 using a sorbent material (Nitra-Zorb™, API).
144 Following nitrate removal, the groundwater was amended with sodium acetate (250 μM),
145 monopotassium phosphate (1 μM), and ammonium chloride (50 μM) to stimulate microbial activity.
146 We also added sodium SO_4^{2-} (500 μM) to potentially support growth of SO_4^{2-} reducers present in the

147 inoculum. Addition of SO_4^{2-} was necessary because, unlike well CHM95A, groundwater from
148 CHM95D contained little SO_4^{2-} (<10 μM). Acetate, the electron donor used by microbes in the
149 experiment, was not added to groundwater used in abiological (control) experiments to help
150 ensure that they remained sterile throughout the study. The amount added to the medium used for
151 biologically-active reactors is higher than that typically observed in natural aquifers. Acetate
152 concentrations in coastal plain aquifers, for example, range up to about 30 μM (McMahon and
153 Chapelle, 1991). However, once acetate consumption reached steady state during the experiments,
154 the maximum concentration of acetate in the reactors at any given time was 50 μM, a value similar
155 to that observed in coastal plain aquifers.
156 After amendments were added, 100 mL of the medium was dispensed into 160 mL serum
157 bottles (Wheaton) and purged for 1 h to remove oxygen. The purge gas consisted either entirely of
158 CO_2 (medium for high-CO_2 reactors; ~1 atm PCO_2) or nitrogen containing 2% CO_2 (medium for low-
159 CO_2 reactors; ~0.02 atm PCO_2). After purging, the bottles were stoppered and sealed as described
160 above, autoclaved for 20 minutes at 121°C, and stored at room temperature (~22°C) until they
161 were used to replenish fluids removed from the reactors during the experiment, as described
162 below. The final composition of the groundwater medium is provided in the Electronic Annex
163 (Table EA1).
164
165 **2.3. Bioreactors**
166 Each set of bioreactor experiments was performed in duplicate: (1) biologically-active and
167 control (abiological) reactors containing high-CO_2 medium and (2) biologically-active and control
168 reactors containing low-CO_2 medium. The reactors consisted of 160 mL serum bottles containing
169 100 mL of groundwater medium and 1 mmol of goethite (α-FeOOH) , which provided a source of
170 Fe(III) for Fe(III) reducers. Preparation and identification of the goethite was described previously

(Kirk et al., 2010). Aquifer sediment was not included because the experiments were intended to isolate the interaction between microbes and CO_2.

Each reactor was plugged with a butyl rubber stopper penetrated by a 4 inch stainless-steel needle (Popper), which was used for fluid exchanges during the experiment. The needle was capped with a gas-tight syringe valve (VICI Precision Sampling) to prevent gas leakage. After the reactors were fully assembled, we sterilized them by autoclaving for 20 minutes at 121°C and then purged them through the 4 inch needle with filter-sterilized CO_2 or 2% CO_2 in nitrogen. Hence, the initial fluid in the reactors had a composition equivalent to the high-CO_2 medium or the low-CO_2 medium. During purging, each septum was also penetrated with a second needle that extended into the reactor headspace and allowed purge gas to escape.

After the reactor solutions were purged and cooled to room temperature, they were inoculated with 1 mL of solution from the CHM95A microbe sample. The sample was vortexed for 30 seconds prior to withdrawing inoculum to dislodge cells from sediment surfaces. The inoculum injected into the control reactors had been sterilized prior to injection by autoclaving 3 times with at least 48 h between sterilizations.

Following incubation for 1 week and every seventh day thereafter, one-fifth (20 mL) of the aqueous volume of each reactor was removed through the fixed needle without disturbing reactor solids. Effluent was withdrawn with a 20 mL syringe (BD), which was sealed with a syringe valve (Cole-Parmer) and used for short-term storage until the water could be analyzed. Lastly, the volume withdrawn was immediately replaced with 20 mL of fresh medium using a syringe and the reactor was gently mixed. This schedule of medium delivery equates to a fluid residence time of 35 days. The reactors incubated in the dark at room temperature during the experiment.

2.4. Chemical analyses

Precision and detection limits of chemical analyses are summarized in the Electronic Annex (Table EA2). Chemical analysis of effluent samples was performed each week. Fe(II) concentration was measured in effluent samples using the ferrozine method (Stookey, 1970) with a Varian Cary 50 UV-Vis spectrophotometer. Total alkalinity was measured using Gran alkalinity titrations with 0.02 N sulfuric acid and a Thermo Orion 410A+ pH meter with a Cole Parmer pH electrode. Acetate, phosphate, and SO_4^{2-} concentration was measured in 0.45 μm filtered samples using a Dionex ICS-1100 ion chromatograph (IC) with an IonPac® AS23 column. Fe(II) and alkalinity analyses were performed immediately after the samples were collected. IC analysis was typically carried out on samples stored overnight at 4°C.

Groundwater medium was periodically analyzed using the same procedures used for reactor effluent. In addition to those methods, four samples were also analyzed for major cation concentrations (Na^+, K^+, Mg^{2+}, Ca^{2+}) using a Perkin Elmer AAnalyst 200 atomic absorption spectrometer (AAS) and Perkin Elmer Optima 8000 inductively coupled plasma optical emission spectrometer (ICP OES).

The acid volatile sulfide (AVS) content of the reactors was measured in samples collected at the end of the experiment to gauge the extent of sulfide mineralization. The analysis was performed as described by Kirk et al. (2010), by reacting fresh, well-mixed bioreactor samples with a hydrochloric acid solution and measuring sulfide concentration using the methylene blue method (Eaton et al., 1995).

2.5. Microbial community analysis

We collected samples for microbial community analysis at the end of the experiment by shaking the reactors to thoroughly mix them and then immediately withdrawing fluid. By this approach, the samples contained both water and solids. Total community DNA was extracted from the samples using an Ultraclean® Microbial DNA Isolation Kit (MO BIO). We performed the

extraction using the "Alternative Lysis Method" described by the manufacturer to limit DNA shearing.

16S rRNA genes in the extract were amplified and sequenced at a commercial laboratory (MR DNA™). PCR amplification was performed using universal bacterial primers 27F (AGRGTTTGATCMTGGCTCAG) and 519R (GTNTTACNGCGGCKGCTG) with HotStarTaq Plus Master Mix (Qiagen, Valencia, CA). The reactions were held 94°C for 3 minutes, followed by 28 cycles of 94°C for 30 seconds, 53°C for 40 seconds, and 72°C for 1 minute. Following the last cycle, a final elongation step at 72°C for 5 minutes was performed. After PCR, amplicon pyrosequencing (bTEFAP) as described by Dowd *et al.* (2008) was used to sequence 16S rRNA genes. Amplicon products from different samples were mixed in equal proportion and purified using AMPure® beads (Agencourt Bioscience Corporation). Samples were sequenced using a Roche 454 FLX titanium instrument and reagents according to manufacturer guidelines.

We processed the sequence data using QIIME (Caporaso et al., 2010). The program used AmpliconNoise (Quince et al., 2011) to remove primers, barcodes, low-quality reads, and chimeras from the sequences. After this step, 10,479 sequences remained (1767 and 2007 from the high-CO_2 reactors and 3545 and 3160 from the low-CO_2 reactors) averaging 352 bp (st. dev. 56.3) in length. QIIME then defined Operational Taxonomic Units (OTUs) at 97% sequence similarity using UCLUST (Edgar, 2010). Taxonomic classification was carried out on representative sequences from each OTU using the Ribosomal Database Project classifier (Wang et al., 2007) (v. 2.2) with an 80% confidence threshold.

2.6. Mass-balance and thermodynamic calculations

Rates of acetate oxidation and Fe(III) and SO_4^{2-} reduction were evaluated using mass-balance calculations as described previously (Bethke et al., 2011; Kirk et al., 2010). A detailed description of those calculations is available in the Electronic Annex. Chemical activities and

mineral saturation indexes were calculated using The Geochemists Workbench® software, version 8.0.10, and the LLNL (Lawrence Livermore National Laboratory) thermodynamic database (Delany and Lundeen, 1990). The software calculated activities using an extended form of the Debye-Hückel equation, the *B*-dot equation (Helgeson, 1969), which is appropriate for solutions with low ionic strength such as the groundwater medium (I <0.02 molal).

To examine whether thermodynamic controls could have affected the rate of Fe(III) and SO_4^{2-} reduction in the bioreactors, we calculated how much energy was available (ΔG_A) to drive the reactions forward. Net metabolic reactions for acetate-consuming Fe(III) and SO_4^{2-} reducers can be expressed as follows:

$$8\,FeOOH + 15\,H^+ + CH_3COO^- \rightarrow 2\,HCO_3^- + 12\,H_2O + 8\,Fe^{2+} \quad (1)$$

$$SO_4^{2-} + CH_3COO^- \rightarrow 2\,HCO_3^- + HS^- \quad (2)$$

where goethite provides the source of Fe(III) for Fe(III) reducers. ΔG_A for each group is the negative of the free energy change (ΔG_r) of each group's net metabolic reaction (Bethke et al., 2011):

$$\Delta G_A = -\Delta G_r = -[\Delta G_T^{\circ} + RT ln \prod_i (\gamma_i \times m_i)^{v_i}] \quad (3)$$

Where $\Delta G°_T$ is the standard Gibbs free-energy change for reaction *r* at temperature *T* (°K), *R* represents the gas constant (kJ·mol^{-1}·K^{-1}), γ_i and m_i are the activity coefficient (molal^{-1}) and molality of the *i*th chemical species in the reaction, and v_i is the stoichiometric coefficient of that species,

which is positive for products and negative for reactants. $\Delta G°_T$ values were calculated using The Geochemists Workbench® software and the LLNL dataset.

Where acetate content was below detection (<19 μM), we report ΔG_A values consistent with that detection limit and describe them as maximum possible values. The reaction for each group was written in terms of the consumption of one acetate. As such, the relative values of ΔG_A we calculated retain some absolute meaning (Bethke et al., 2011). In a single reactor where ≤50 kJ mol^{-1} of energy is available for one group and only ≤20 kJ mol^{-1} for another, for example, the first group would actually see 30 kJ mol^{-1} more energy than the second because inserting an actual acetate concentration in the calculation would change ΔG_A values for each group by an equivalent amount. For comparisons made between reactors, the possibility that acetate levels differ by up to 19 μM adds uncertainty, but the uncertainty is small because, written in terms of one acetate, the ΔG_A of the reactions does not vary strongly with acetate content. All else being equal, for example, if acetate content differed by 19 μM between two of the reactors, the ΔG_A of Fe(III) reduction in each would only differ by 7 kJ mol^{-1}.

3. RESULTS AND DISCUSSION

3.1. Aqueous chemistry

The chemical composition of effluent differed considerably between the high- and low-CO_2 reactors, reflecting differences in CO_2 abundance as well as microbial reaction rates. Consistent with CO_2 partial pressures, the pH of effluent from the high- and low-CO_2 control reactors averaged 5.72 and 7.21, respectively, throughout the experiment (Fig. 1). The pH of effluent from the biologically-active low-CO_2 reactors did not vary significantly from the pH of corresponding control reactors ($P = 0.13$; Student's t-test). The pH of effluent from the biologically-active high-CO_2 reactors, however, did diverge significantly from control pH ($P < 0.0001$). Initially near control

levels, the pH of effluent from both high-CO_2 reactors increased and ultimately stabilized at an average of 5.92 over the final 50 days of the experiment.

This shift in pH occurred simultaneously with changes in effluent acetate, alkalinity, Fe(II), and SO_4^{2-} concentration in the biologically-active reactors (Fig. 1). Acetate content fell from an average of 0.27 mM to values near or below the detection limit (19 μM) by 50 days into the experiment in both sets of reactors. Alkalinity increased from 4.8 meq L^{-1} to an average of 8.4 meq L^{-1} and 5.4 meq L^{-1} during the second half of the experiment in the high- and low-CO_2 reactors, respectively, and Fe(II) content increased from below detection (<1.5 μM) to an average of 1.62 mM and 0.13 mM, respectively. SO_4^{2-} concentration decreased from 0.47 mM to 0.30 mM by the end of the experiment in the low-CO_2 reactors but was not significantly different from control values in the high-CO_2 reactors ($P = 0.37$).

These changes in aqueous chemistry are consistent with growth of Fe(III)- and SO_4^{2-}-reducing microorganisms. Within the first two weeks of the experiment, the decrease in effluent acetate and SO_4^{2-} levels and the increase in Fe(II) and alkalinity content indicate populations of both groups began to grow. Stabilization of effluent acetate content near or below the detection limit during the final 50 days of the experiment indicates that populations in both sets of reactors had grown enough to consume nearly all of the influent acetate each week.

Mass-balance calculations based on aqueous chemistry demonstrate that the extent to which Fe(III) and SO_4^{2-} reduction occurred differed considerably between each set of reactors (Fig. 2). During the final 50 days of the experiment, Fe(III) reduction consumed an average of 90% of the acetate entering the high-CO_2 reactors each week while SO_4^{2-} reduction consumed a negligible amount (<1%). In contrast, over that same interval in the low-CO_2 experiment, Fe(III) reduction consumed an average of only 15% of the acetate supply each week while SO_4^{2-} reducers consumed 85%. The sum of acetate consumption by Fe(III) and SO_4^{2-} reduction does not total 100% for the high-CO_2 reactors possibly because the values are averages over time and between duplicate

316 reactors. Adsorption of Fe(II) to surfaces within the reactors may have also contributed to this
317 discrepancy by causing the rate of Fe(III) reduction to be underestimated (see description of mass-
318 balance calculations in Electronic Annex). Nonetheless, the results of the calculation provide strong
319 evidence that higher CO_2 abundance increased the ability of Fe(III) reducers to compete with SO_4^{2-}
320 reducers in the reactors.
321
322 **3.2. Microbial community composition**
323 Results from analysis of 16S rRNA genes obtained from each reactor are consistent with the
324 mass-balance calculations (Fig. 3). Lineages that contain organisms capable of using Fe(III) as their
325 electron acceptor were present in the samples from both sets of reactors. In high-CO_2 reactor
326 samples, an average of 25% and 24% of the sequences grouped within *Geobacteraceae* and
327 *Myxococcaceae*, respectively, which contain groups capable of dissimilatory Fe(III) reduction such
328 as *Geobacter* (Lonergan et al., 1996) and *Anaeromyxobacter* (Treude et al., 2003), respectively. In
329 samples from the low-CO_2 reactors, few sequences grouped within *Myxococcaceae* (<1%) but
330 sequences grouping within *Geobacteraceae* accounted for 22% of the sequences on average. Hence,
331 sequences from groups containing organisms capable of Fe(III) reduction were abundant in all four
332 biologically-active reactors but more than twice as abundant in the high-CO_2 reactor samples as the
333 low-CO_2 reactor samples on average.
334 Also consistent with the mass-balance calculations, SO_4^{2-} reducing groups were much more
335 abundant in the low-CO_2 reactors than the high-CO_2 reactors (Fig. 3). Sequences grouping in
336 families with organisms that commonly use SO_4^{2-} as their electron acceptor [*Desulfobulbaceae*,
337 *Desulfovibrionaceae*, *Desulfuromonadaceae*, *Desulfobacteraceae*, *Syntrophaceae*, and
338 *Syntrophobacteraceae* (Garrity et al., 2005)] accounted for an average of 20% of the sequences in
339 low-CO_2 reactor samples but were nearly absent in high-CO_2 reactor samples (<1%).

The microbial community we observed in the low-CO_2 reactors is similar to that observed in the aquifer used as a source of inoculum and groundwater. As noted above, Fe(III) and SO_4^{2-} reducers coexist in the aquifer where SO_4^{2-} is sufficiently available, a relationship also observed in many other anoxic environments (Postma and Jakobsen, 1996). Like the low-CO_2 reactors, furthermore, *δ-Proteobacteria* are common in the aquifer (Flynn et al., 2013; Flynn et al., 2012).

In contrast, the abundance of sequences from the high-CO_2 reactors that grouped in *Myxococcaceae* is unlike the Mahomet aquifer. This difference may reflect a preference of Fe(III)-reducing *Anaeromyxobacter* species for growth at acidic pH, as indicated by previous research (Petrie et al., 2003; Thomas et al., 2009). Whereas the pH of water in the high-CO_2 reactors was acidic, the pH of Mahomet aquifer groundwater is typically slightly basic (Flynn et al., 2012).

3.3. Controls on reaction rates

The results of our thermodynamic calculations demonstrate that variation in ΔG_A may have contributed to differences in reaction rates between each set of reactors. Values of ΔG_A we calculated differed considerably between the high- and low-CO_2 reactors for Fe(III) reduction but varied little between each set of reactors for SO_4^{2-} reduction (Fig. 4). ΔG_A for Fe(III) reduction was a maximum of 114 kJ mol^{-1} on average over the final 50 days in the high-CO_2 reactors compared to only a maximum of 60 kJ mol^{-1} in the low-CO_2 reactors. During that same interval, ΔG_A for SO_4^{2-} reduction was a maximum of 65 kJ mol^{-1} and 62 kJ mol^{-1} on average in the high- and low-CO_2 reactors, respectively.

The lack of variation in ΔG_A for SO_4^{2-} reduction indicates that thermodynamic controls did not directly cause variation in SO_4^{2-} reduction rates between each set of reactors. Variation in ΔG_A for Fe(III) reduction, however, is consistent with thermodynamic controls as a cause of variation. A series of studies by Jin and Bethke (2002, 2003, 2005, 2007, 2009) has shown that energy available for a microbial reaction can be a dominant control on the rate at which that reaction can occur.

Those authors found that, where ΔG_A is high relative to the amount of energy conserved by a cells metabolism, thermodynamic controls do not directly limit reaction rates. Where ΔG_A approaches the amount conserved, however, rates grow increasingly limited by thermodynamic controls. Fe(III) reduction may have occurred more rapidly in the high-CO_2 reactors than the low-CO_2 reactors, therefore, because ΔG_A was higher in the high-CO_2 reactors. Although ΔG_A for SO_4^{2-} reducers varied little, furthermore, an increase in the ability of Fe(III) reducers to compete for acetate as a result of their increase in ΔG_A may explain the low level of SO_4^{2-} reduction in the high-CO_2 reactors.

Variation in ΔG_A for each group is consistent with the relationship between free energy and pH noted in the Introduction. The energy yield of microbial Fe(III) reduction increases sharply as pH decreases because the reaction consumes a large number of protons (equation 1). As such, the reaction was much more favorable at the lower pH of the high-CO_2 reactors than the near-neutral pH of the low-CO_2 reactors. In contrast, the energy yield of SO_4^{2-} reduction varies little with pH because the reaction consumes few protons (equation 2). ΔG_A for SO_4^{2-} reduction varied little between each set of reactors. CO_2 may have influenced reaction rates in the bioreactors not by causing variation in the concentration of dissolved inorganic carbon species, therefore, but by affecting pH.

The observed variation in the balance between Fe(III) and SO_4^{2-} reduction with pH is consistent with the findings of Postma and Jakobsen (1996). Based on a thermodynamic analysis and geochemical evidence from multiple field sites, they concluded that Fe(III) reduction and SO_4^{2-} reduction may proceed simultaneously over a wide range of conditions but that Fe(III) reduction is favored at acidic pH. In general, however, many factors besides thermodynamics can affect the rate of a microbial reaction, including the abundance of cells and the kinetics of electron donation and acceptance (Jin and Bethke, 2007). In addition to affecting ΔG_A, a lower pH caused by CO_2 could have also affected reaction rates by influencing cell physiology. Cells have a pH range within which

growth is possible and usually an optimum pH, at which growth rates are maximized (Madigan et al., 2003). Hence, CO_2-driven shifts in pH away from the pH optima may have contributed to differences in reaction rates. Moreover, the toxic effects imposed by CO_2 itself, as discussed in the Introduction, may have also contributed to variation in reaction rates if the Fe(III) reducers in the experiment were less sensitive to CO_2 toxicity than the SO_4^{2-} reducers. Additional research is warranted to fully examine the influence of CO_2 on thermodynamic and kinetic controls on microbial reaction rates as well as the extent to which different groups of microorganism are sensitive to its toxic effects.

3.4. Impact on CO_2 trapping

Solubility trapping occurs when CO_2 dissolves into pore water. The amount that can dissolve varies directly with the partial pressure of CO_2. More CO_2 was trapped within the aqueous phase of the high-CO_2 reactors than the low-CO_2 reactors, therefore, because more CO_2 was present in the headspace of the high-CO_2 reactors. Differences in the amount of inorganic carbon stored in solution widened, however, as a result of the high rate of Fe(III) reduction in the high-CO_2 reactors.

Because Fe(III) reduction consumes a large number of protons (equation 1), the reaction can generate a large amount of carbonate alkalinity by driving conversion of dissolved CO_2 into bicarbonate:

$$CO_2(aq) + H_2O \rightarrow H^+ + HCO_3^- \quad (4)$$

Where this occurs, additional CO_2 can then dissolve in place of that converted to alkalinity, thereby increasing the amount of inorganic carbon stored in solution. Combining equation (4) with the net metabolic reaction for Fe(III) reducers (1) illustrates this relationship:

$$CH_3COO^- + 8\,FeOOH + 15\,CO_2(aq) + 3\,H_2O \rightarrow 17\,HCO_3^- + 8\,Fe^{2+} \quad (5)$$

Comparing (5) to the equation listed above for sulfate reduction (2), we see that Fe(III) reduction can generate up to 8 times more carbonate alkalinity than SO_4^{2-} reduction per mole of acetate oxidized. Although microbial activity increased carbonate alkalinity in both sets of reactors, therefore, solubility trapping was enhanced to a greater extent in the high-CO_2 reactors because they hosted more rapid Fe(III) reduction.

The increase in alkalinity that occurred in the high-CO_2 reactors was 6 times greater than that in the low-CO_2 reactors, a value similar to that predicted by the stoichiometry above. Differences between these values may reflect variation in aqueous speciation. Writing SO_4^{2-} reduction in terms of dihydrogen sulfide instead of bisulfide causes the reaction to yield an additional mole of alkalinity per mole of acetate consumed. Moreover, additional reactions occurring in the experiment besides Fe(III) reduction and SO_4^{2-} reduction may have also affected alkalinity, including mineral precipitation and surface complexation.

In addition to impacting solubility trapping, saturation state calculations show that the shift toward a higher rate of Fe(III) reduction also favored enhanced mineral trapping of CO_2. Mineral trapping occurs where carbonate ions form from CO_2 and precipitate as a carbonate mineral such as siderite ($FeCO_3$) or calcite ($CaCO_3$). Precipitation of calcite was unfavorable on average in both sets of reactors (Fig. 5). The average saturation index (log Q/K) of calcite over the last 50 days of the experiment was -1.1 and -0.1 in the high- and low-CO_2 reactors, respectively. Increases in pH, Fe(II), and alkalinity levels caused by microbial activity, however, caused siderite to become supersaturated within the first two weeks in both sets of reactors. The average saturation index of siderite over the last 50 days was 0.9 and 0.8 in the high- and low-CO_2 reactors, respectively. While siderite was supersaturated in both sets of experiments, given enough time, more siderite may have formed in the high-CO_2 experiments because more Fe(II) and bicarbonate alkalinity were available.

Based on our mass-balance calculations, 5 times more Fe(II) was produced in the high-CO_2 reactors as the low-CO_2 reactors.

We have no direct evidence that siderite formed in our reactors. It is certainly possible that none did considering that siderite precipitation occurs slowly at room temperature (Jimenez-Lopez and Romanek, 2004). Nonetheless, it is useful to note this shift in the potential for siderite to precipitate because CO_2 storage and leakage would occur over much longer time scales than our experiments if geological carbon storage is implemented. Hence, minerals that form slowly may not have formed in our experiments but could be important over longer time scales in natural environments.

3.5. Impact on water quality

In contrast to the benefit of enhanced CO_2 trapping, the elevated rate of Fe(III) reduction in the high-CO_2 reactors negatively impacted water quality. The secondary water standard recommended by the U.S. EPA for Fe in drinking water is 5 μM. This level was easily exceeded in both sets of reactors (Fig. 1). The extent to which Fe(II) accumulated in solution was far greater, however, in the high-CO_2 reactors.

Coupled with this impact, AVS measurements and mass-balance calculations show that an increased rate of Fe(III) reduction also led to lower abundances of goethite and solid-phase sulfide. Reflecting the balance between Fe(III) and SO_4^{2-} reduction, the abundance of goethite and AVS was considerably lower in the high-CO_2 reactors than the low-CO_2 reactors at the end of the experiment. Our mass-balance calculations indicate that goethite content averaged 0.9 mmol in the biologically-active low-CO_2 reactors compared to only 0.5 mmol in the biologically-active high-CO_2 reactors at the end of the experiment. Similarly, AVS content averaged 35.7 μmol in the biologically-active low-CO_2 reactors compared to only 1.4 μmol in the biologically-active high-CO_2 reactors (Fig. 6). The

463 AVS that formed likely consisted of mackinawite (~FeS), the precursor to pyrite in Fe-bearing, SO_4^{2-}
464 reducing environments (Berner, 1970).

465 These differences in mineralogy have the potential to affect water quality because both
466 solid-phases provide important sinks for many hazardous solutes in aqueous environments.
467 Arsenic, for example, can strongly sorb to iron oxides and oxyhydroxides or be sequestered by
468 sulfide minerals (Smedley and Kinniburgh, 2002). The CO_2-induced shifts in microbiology that we
469 observed, therefore, favor enhance mobility of hazardous solutes such as arsenic.
470

471 **3.6. Implications for geological carbon storage**

472 Our findings imply that CO_2 leakage into Fe-bearing anoxic aquifers can stimulate microbial
473 Fe(III) reduction. Where this occurs, CO_2 trapping would be enhanced but water quality could
474 decrease. Because of these relationships, numerical simulations aiming to predict the long-term
475 behavior of CO_2 leakage may underestimate the rate of CO_2 trapping and the negative impact on
476 water quality if they do not account for microbial activity. Furthermore, these findings also imply
477 that CO_2 leakage into an anoxic aquifer is less likely to reach the surface if Fe(III) and an active
478 microbial community are present.

479 Whether the results of this study also have implications for deep CO_2 reservoirs is unclear.
480 The redox state of deep subsurface environments is often similar to that in our experiments, with
481 Fe(III), SO_4^{2-}, and inorganic carbon existing as the primary electron acceptors available (Bethke et
482 al., 2011; Lovley and Chapelle, 1995). Hence, a similar microbial feedback is possible. However, the
483 conditions would differ considerably from this experiment in terms of temperature, total pressure,
484 and salinity. The amount of CO_2 the microbial community could be exposed to could also range to
485 much higher levels. Additional research is needed, therefore, to evaluate whether this feedback can
486 exist under conditions consistent with the deep subsurface.
487

4. CONCLUSIONS

Our results demonstrate that the ability of Fe(III) reducers to compete with SO_4^{2-} reducers was enhanced in reactors with high CO_2 content. Whereas SO_4^{2-} reducers accounted for most of the acetate consumption in the low-CO_2 reactors, Fe(III) reducers were dominant in the high-CO_2 reactors. Free energy calculations show that this shift may reflect variation in thermodynamic controls on microbial Fe(III) reduction. Physiological effects and CO_2 toxicity may have also contributed to differences in microbial activity.

This shift in microbial activity impacted both carbon storage and water quality in the reactors. As a result of more rapid Fe(III) reduction, solubility trapping was enhanced and conditions were more favorable for siderite precipitation. Hence, the shift toward Fe(III) reduction that we observed at higher CO_2 abundance represents a microbial feedback mechanism on CO_2 trapping. However, the increased rate of Fe(III) reduction diminished water quality by greatly increasing Fe(II) concentration and led to lower abundances of goethite and solid-phase sulfide, solids that commonly serve as important sinks for hazardous solutes. Because the interactions between CO_2 and microorganisms that we observed are possible in natural environments, accounting for microbial activity may improve the ability of numerical simulations to predict the fate and environmental impact of CO_2 in the subsurface.

ACKNOWLEDGEMENTS

We are extremely grateful for laboratory support from Christopher Marry, Scot Dowd, Thomas Stewart, Andrew Miller, and Ernesto Tellez, helpful comments from Qusheng Jin, and a thorough manuscript review by Amy Halloran and three anonymous reviewers. This material is based upon work supported as part of the Center for Frontiers of Subsurface Energy Security, an Energy Frontier Research Center funded by the U.S. Department of Energy, Office of Science, Office of Basic Energy Sciences under Award Number DE-SC0001114. Sandia National Laboratories is a

multi-program laboratory managed and operated by Sandia Corporation, a wholly owned subsidiary of Lockheed Martin Corporation, for the U.S. Department of Energy's National Nuclear Security Administration under contract DE-AC04-94AL85000.

References

Apps, J. A., Zheng, L., Zhang, Y., Xu, T., Birkholzer, J. T. (2010) Evaluation of potential changes in groundwater quality in response to CO_2 leakage from deep geologic storage. *Transport Porous Med.* **82**, 215-246.

Benson, S. M., Cole, D. R. (2008) CO_2 sequestration in deep sedimentary formations. *Elements* **4**, 325-331.

Benzerara, K., Miot, J., Morin, G., Ona-Nguema, G., Skouri-Panet, F., Ferard, C. (2011) Significance, mechanisms and environmental implications of microbial biomineralization. *C. R. Geosci.* **343**, 160-167.

Berner, R. A. (1970) Sedimentary pyrite formation. *Am. J. Sci.* **268**, 1-23.

Bertoloni, G., Bertucco, A., De Cian, V., Parton, T. (2006) A study on the inactivation of micro-organisms and enzymes by high pressure CO_2. *Biotechnol. Bioeng.* **95**, 155-160.

Bethke, C. M., Sanford, R. A., Kirk, M. F., Jin, Q., Flynn, T. M. (2011) The thermodynamic ladder in geomicrobiology. *Am. J. Sci.* **311**, 183-210.

Burch, S. L. (2008) Development of an Observation Well Network in the Mahomet Aquifer of East-Central Illinois, Data/Case Study 2008-01. Illinois State Water Survey, Champaign, IL, p. 111.

Caporaso, J. G., Kuczynski, J., Stombaugh, J., Bittinger, K., Bushman, F. D., Costello, E. K., Fierer, N., Pena, A. G., Goodrich, J. K., Gordon, J. I., Huttley, G. A., Kelley, S. T., Knights, D., Koenig, J. E., Ley, R. E., Lozupone, C. A., McDonald, D., Muegge, B. D., Pirrung, M., Reeder, J., Sevinsky, J. R., Tumbaugh, P. J., Walters, W. A., Widmann, J., Yatsunenko, T., Zaneveld, J., Knight, R. (2010) QIIME allows analysis of high-throughput community sequencing data. *Nat. Methods* **7**, 335-336.

Celia, M. A., Nordbotten, J. M. (2009) Practical modeling approaches for geological storage of carbon dioxide. *Ground Water* **47**, 627-638.

Delany, J. M., Lundeen, S. R. (1990) The LLNL thermochemical database, LLNL report UCRL-21658. Lawrence Livermore National Laboratory.

Dowd, S. E., Callaway, T. R., Wolcott, R. D., Sun, Y., McKeehan, T., Hagevoort, R. G., Edrington, T. S. (2008) Evaluation of the bacterial diversity in the feces of cattle using 16S rDNA bacterial tag-encoded FLX amplicon pyrosequencing (bTEFAP). *BMC Microbiol.* **8**.

Eaton, A. D., Clesceri, L. S., Greenberg, A. E. (1995) *Standard Methods for the Examination of Water and Wastewater*, 19 ed. American Public Health Association, American Water Works Association, and Water Environmental Federation, Washington, DC USA.

Edgar, R. C. (2010) Search and clustering orders of magnitude faster than BLAST. *Bioinformatics* **26**, 2460-2461.

Flynn, T. M., Sanford, R. A., Bethke, C. M. (2008) Attached and suspended microbial communities in a pristine confined aquifer. *Wat. Resour. Res.* **44**, 1-7.

Flynn, T. M., Sanford, R. A., Ryu, H., Bethke, C. M., Levine, A. D., Ashbolt, N. J., Santo Domingo, J. W. (2013) Functional microbial diversity explains groundwater chemistry in a pristine aquifer. *BMC Microbiol.* **13**.

Flynn, T. M., Sanford, R. A., Santo Domingo, J. W., Ashbolt, N. J., Levine, A. D., Bethke, C. M. (2012) The active bacterial community in a pristine confined aquifer. *Wat. Resour. Res.* **48**, W09510.

Garrity, G. M., Brenner, D. J., Krieg, N. R., Staley, J. T. (2005) The *Alpha-*, *Beta-*, *Delta-*, and *Epsilonproteobacteria*, Bergey's Manual of Systematic Bacteriology. Springer, New York.

Gerlach, R., Cunningham, A. B. (2010) Influence of Biofilms on Porous Media Hydrodynamics, in: Vafai, K. (Ed.), *Porous Media: Applications in Biological Systems and Biotechnology*. CFC Press, New York, pp. 173-230.

Harvey, O. R., Qafoku, N. P., Cantrell, K. J., Lee, G., Amonette, J. E., Brown, C. F. (2013) Geochemical implications of gas leakage associated with geological CO_2 storage - a qualitative review. *Environ. Sci. Technol.* **47**, 23-36.

Helgeson, H. C. (1969) Thermodynamics of hydrothermal systems at elevated temperatures and pressures. *Am. J. Sci.* **267**, 729-804.

Inagaki, F., Kuypers, M. M. M., Tsunogai, U., Ishibashi, J., Nakamura, K., Treude, T., Ohkubo, S., Nakaseama, M., Gena, K., Chiba, H., Hirayama, H., Nunoura, T., Takai, K., Jorgensen, B. B., Horikoshi, K., Boetius, A. (2006) Microbial community in a sediment-hosted CO_2 lake of the southern Okinawa Trough hydrothermal system. *P. Natl. Acad. Sci. USA* **103**, 14164-14169.

IPCC (2005) Special Report on Carbon Capture and Storage. Available at http://www.ipcc.ch/.

Jimenez-Lopez, C., Romanek, C. S. (2004) Precipitation kinetics and carbon isotope partitioning of inorganic siderite at 25°C and 1 atm. *Geochim. Cosmochim. Acta* **68**, 557-571.

Jin, Q., Bethke, C. M. (2002) Kinetics of electron transfer through the respiratory chain. *Biophys. J.* **83**, 1797-1808.

Jin, Q., Bethke, C. M. (2003) A new rate law describing microbial respiration. *Appl. Environ. Microbiol.* **69**, 2340-2348.

Jin, Q., Bethke, C. M. (2005) Predicting the rate of microbial respiration in geochemical environments. *Geochim. Cosmochim. Acta* **69**, 1133-1143.

Jin, Q., Bethke, C. M. (2007) The thermodynamics and kinetics of microbial metabolism. *Am. J. Sci.* **307**, 643-677.

Jin, Q., Bethke, C. M. (2009) Cellular energy conservation and the rate of microbial sulfate reduction. *Geology* **37**, 1027-1030.

Kelly, W. R., Holm, T. R., Wilson, S. D., Roadcap, G. S. (2005) Arsenic in glacial aquifers: sources and geochemical controls. *Ground Water* **43**, 500-510.

Kempton, J. P., Johnson, W. H., Heigold, P. C., Cartwright, K. (1991) Mahomet Bedrock Valley in east-central Illinois; Topography, glacial drift stratigraphy, and hydrogeology, in: Melhorn, W.N., Kempton, J.P. (Eds.), *Geology and hydrogeology of the Teays-Mahomet Bedrock Valley System*. Geological Society of America Special Paper 258, pp. 91-124.

Kharaka, Y. K., Thordsen, J. J., Kakouros, E., Ambats, G., Herkelrath, W. N., Beers, S. R., Birkholzer, J. T., Apps, J. A., Spycher, N. F., Zheng, L. E., Trautz, R. C., Rauch, H. W., Gullickson, K. S. (2010) Changes in the chemistry of shallow groundwater related to the 2008 injection of CO_2 at the ZERT field site, Bozeman, Montana. *Environ. Earth Sci.* **60**, 273-284.

Kirk, M. F. (2011) Variation in energy available to populations of subsurface anaerobes in response to geological carbon storage. *Environ. Sci. Technol.* **45**, 6676-6682.

Kirk, M. F., Roden, E. E., Crossey, L. J., Brearley, A. J., Spilde, M. N. (2010) Experimental analysis of arsenic precipitation during microbial sulfate and iron reduction in model aquifer sediment reactors. *Geochim. Cosmochim. Acta* **74**, 2538-2555.

Little, M. G., Jackson, R. B. (2010) Potential impacts of leakage from deep CO_2 geosequestration on overlying freshwater aquifers. *Environ. Sci. Technol.* **44**, 9225-9232.

Lonergan, D. J., Jenter, H. L., Coates, J. D., Phillips, E. J. P., Schmidt, T. M., Lovley, D. R. (1996) Phylogenetic analysis of dissimilatory Fe(III)-reducing bacteria. *J. Bacteriol.* **178**, 2402-2408.

Lovley, D. R. (2001) Bioremediation - Anaerobes to the rescue. *Science* **293**, 1444-1446.

Lovley, D. R., Chapelle, F. H. (1995) Deep subsurface microbial processes. *Rev. Geophys.* **33**, 365-381.

607 Lu, J. M., Partin, J. W., Hovorka, S. D., Wong, C. (2010) Potential risks to freshwater resources as a
608 result of leakage from CO_2 geological storage: a batch-reaction experiment. *Environ. Earth*
609 *Sci.* **60**, 335-348.
610 Madigan, M. T., Martinko, J. M., Parker, J. (2003) *Brock Biology of Microorganisms*, 10 ed. Pearson
611 Education, Inc., Upper Saddle River.
612 McMahon, P. B., Chapelle, F. H. (1991) Microbial production of organic acids in aquitard sediments
613 and its role in aquifer geochemistry. *Nature* **349**, 233-235.
614 Mitchell, A. C., Phillips, A. J., Hamilton, M. A., Gerlach, R., Hollis, W. K., Kaszuba, J. P., Cunningham, A.
615 B. (2008) Resilience of planktonic and biofilm cultures to supercritical CO_2. *J. Supercrit.*
616 *Fluids* **47**, 318-325.
617 Oppermann, B. I., Michaelis, W., Blumenberg, M., Frerichs, J., Schulz, H. M., Schippers, A., Beaubien, S.
618 E., Kruger, M. (2010) Soil microbial community changes as a result of long-term exposure to
619 a natural CO_2 vent. *Geochim. Cosmochim. Acta* **74**, 2697-2716.
620 Oule, M. K., Tano, K., Bernier, A. M., Arul, J. (2006) *Escherichia coli* inactivation mechanism by
621 pressurized CO_2. *Can. J. Microbiol.* **52**, 1208-1217.
622 Petrie, L., North, N. N., Dollhopf, S. L., Balkwill, D. L., Kostka, J. E. (2003) Enumeration and
623 characterization of iron(III)-reducing microbial communities from acidic subsurface
624 sediments contaminated with uranium(VI). *Appl. Environ. Microbiol.* **69**, 7467-7479.
625 Postma, D., Jakobsen, R. (1996) Redox zonation: Equilibrium constraints on the Fe(III)/SO_4-
626 reduction interface. *Geochim. Cosmochim. Acta* **60**, 3169-3175.
627 Quince, C., Lanzen, A., Davenport, R. J., Turnbaugh, P. J. (2011) Removing noise from pyrosequenced
628 amplicons. *BMC Bioinformatics* **12**.
629 Santillan, E. U., Kirk, M. F., Altman, S. J., Bennett, P. C. (2013) Mineral influence on microbial survival
630 during carbon sequestration. *Geomicrobiol. J.* **30**, 578-592.
631 Smedley, P. L., Kinniburgh, D. G. (2002) A review of the source, behaviour, and distribution of
632 arsenic in natural waters. *Appl. Geochem.* **17**, 517-568.
633 Stookey, L. L. (1970) Ferrozine - a new spectrophotometric reagent for iron. *Anal. Chem.* **42**, 779-
634 781.
635 Thomas, S. H., Padilla-Crespo, E., Jardine, P. M., Sanford, R. A., Loffler, F. E. (2009) Diversity and
636 distribution of *Anaeromyxobacter* strains in a uranium-contaminated subsurface
637 environment with a nonuniform groundwater flow. *Appl. Environ. Microbiol.* **75**, 3679-3687.
638 Treude, N., Rosencrantz, D., Liesack, W., Schnell, S. (2003) Strain FAc12, a dissimilatory iron-
639 reducing member of the *Anaeromyxobacter* subgroup of *Myxococcales*. *FEMS Microbiol. Ecol.*
640 **44**, 261-269.
641 Uroz, S., Calvaruso, C., Turpault, M. P., Frey-Klett, P. (2009) Mineral weathering by bacteria: ecology,
642 actors and mechanisms. *Trends Microbiol.* **17**, 378-387.
643 Videmsek, U., Hagn, A., Suhadolc, M., Radl, V., Knicker, H., Schloter, M., Vodnik, D. (2009) Abundance
644 and diversity of CO_2-fixing bacteria in grassland soils close to natural carbon dioxide
645 springs. *Microb. Ecol.* **58**, 1-9.
646 Wang, Q., Garrity, G. M., Tiedje, J. M., Cole, J. R. (2007) Naive Bayesian classifier for rapid assignment
647 of rRNA sequences into the new bacterial taxonomy. *Appl. Environ. Microbiol.* **73**, 5261-
648 5267.
649 Wang, S., Jaffe, P. R. (2004) Dissolution of a mineral phase in potable aquifers due to CO_2 releases
650 from deep formations; effect of dissolution kinetics. *Energ. Convers. Manage.* **45**, 2833-2848.
651 Wilkin, R. T., Digiulio, D. C. (2010) Geochemical impacts to groundwater from geologic carbon
652 sequestration: Controls on pH and inorganic carbon concentrations from reaction path and
653 kinetic modeling. *Environ. Sci. Technol.* **44**, 4821-4827.
654 Wimmer, Z., Zarevucka, M. (2010) A review on the effects of supercritical carbon dioxide on enzyme
655 activity. *Int. J. Mol. Sci.* **11**, 233-253.

656 Wu, B., Shao, H. B., Wang, Z. P., Hu, Y. D., Tang, Y. J. J., Jun, Y. S. (2010) Viability and metal reduction
657 of *Shewanella oneidensis* MR-1 under CO_2 stress: Implications for ecological effects of CO_2
658 leakage from geologic CO_2 sequestration. *Environ. Sci. Technol.* **44**, 9213-9218.
659 Yakimov, M. M., Giuliano, L., Crisafi, E., Chernikova, T. N., Timmis, K. N., Golyshin, P. N. (2002)
660 Microbial community of a saline mud volcano at San Biagio-Belpasso, Mt. Etna (Italy).
661 *Environ. Microbiol.* **4**, 249-256.
662 Zhang, J., Davis, T. A., Matthews, M. A., Drews, M. J., LaBerge, M., An, Y. H. H. (2006) Sterilization
663 using high-pressure carbon dioxide. **38**, 354-372.
664 Zheng, L. G., Apps, J. A., Zhang, Y. Q., Xu, T. F., Birkholzer, J. T. (2009) On mobilization of lead and
665 arsenic in groundwater in response to CO_2 leakage from deep geological storage. *Chem. Geol.*
666 **268**, 281-297.

667

668

669 **Figure Captions**

670 **Figure 1**

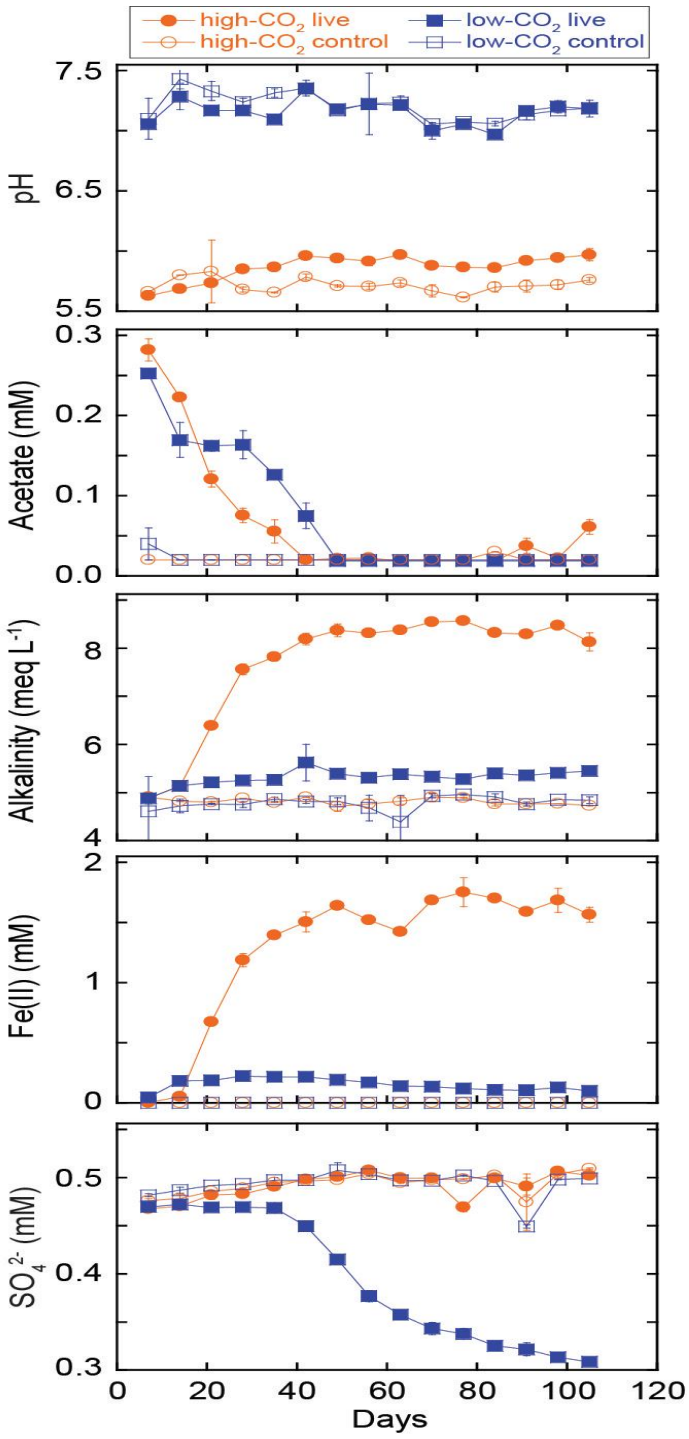

671

672 Figure 1. Variation in the pH, acetate, alkalinity, Fe(II), and SO_4^{2-} content of effluent from the high- and low-
673 CO_2 reactors during the experiment. Control reactors were not biologically active. Each data point shows the
674 median of values measured in duplicate reactors and error bars show the range in values for those duplicates.
675 Detection limits are plotted for values determined to be below method detection limits. Note that the y-axis
676 origin is not zero for graphs showing pH, alkalinity, and SO_4^{2-} data.

677 **Figure 2**

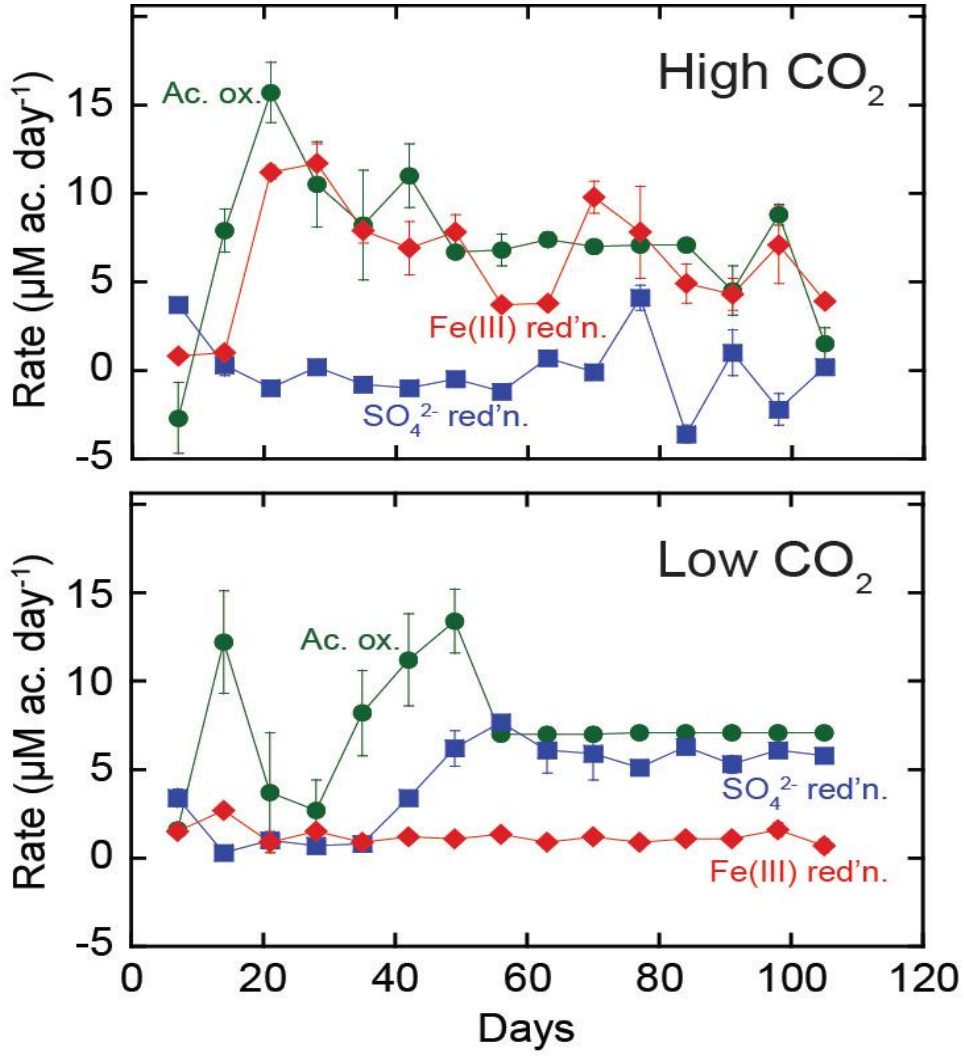

678

679

680 Figure 2. Variation in the overall rate of acetate oxidation and the rate of acetate oxidation by Fe(III) and SO_4^{2-}
681 reducers in the high- and low-CO_2 reactors during the experiment. Each data point shows the median value
682 calculated for duplicate reactors and error bars show the range in values for those duplicates.

683 **Figure 3**

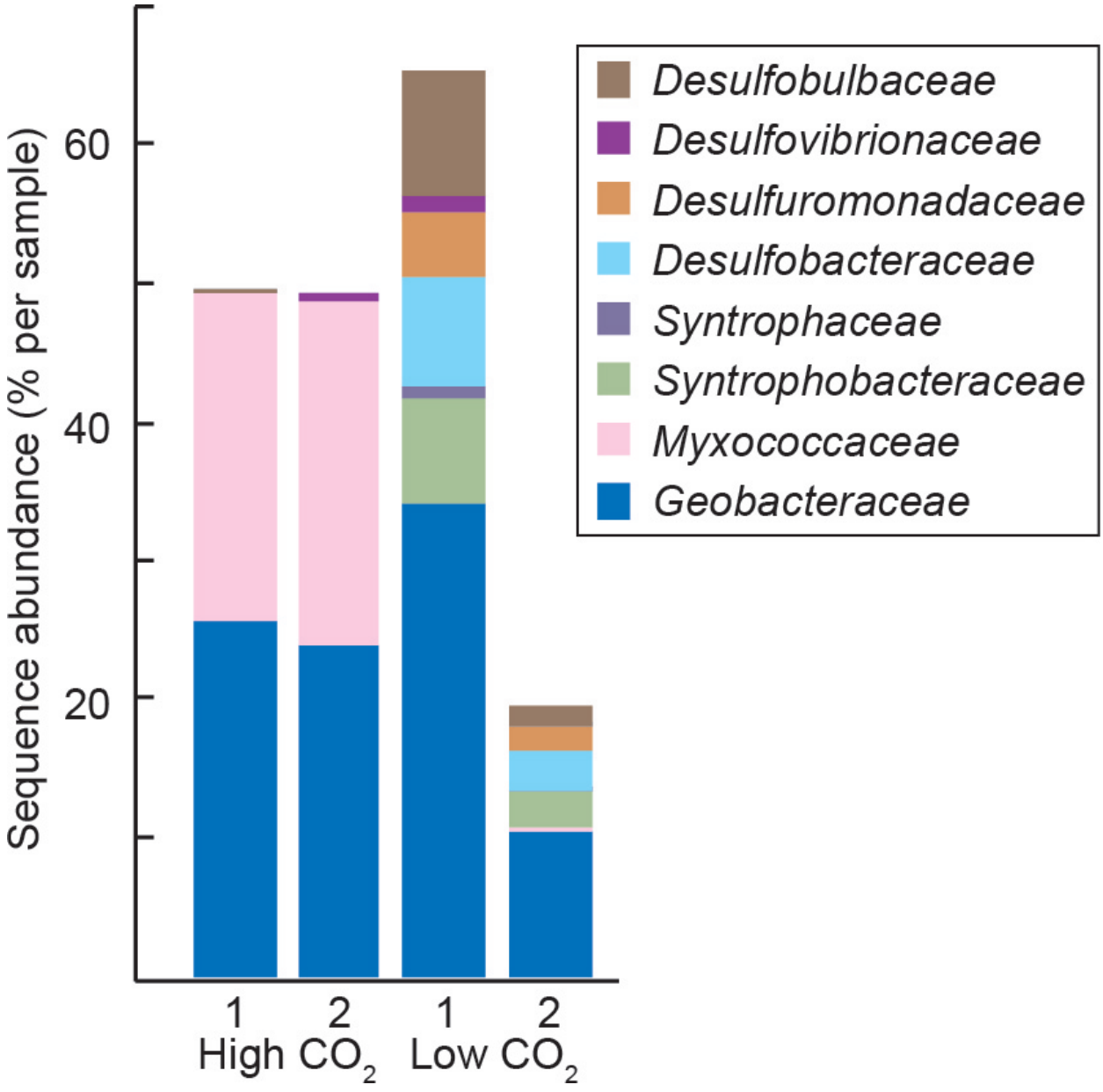

684

685 Figure 3. Taxonomic distribution of sequences grouping within the *δ-Proteobacteria*. Results are shown
686 individually for each duplicate biologically-active reactor. Taxonomy was evaluated at an 80% confidence
687 threshold. An OTU heatmap showing a broader range of taxa than this figure is available in the Electronic
688 Annex (Figure EA2).

689

690

Figure 4

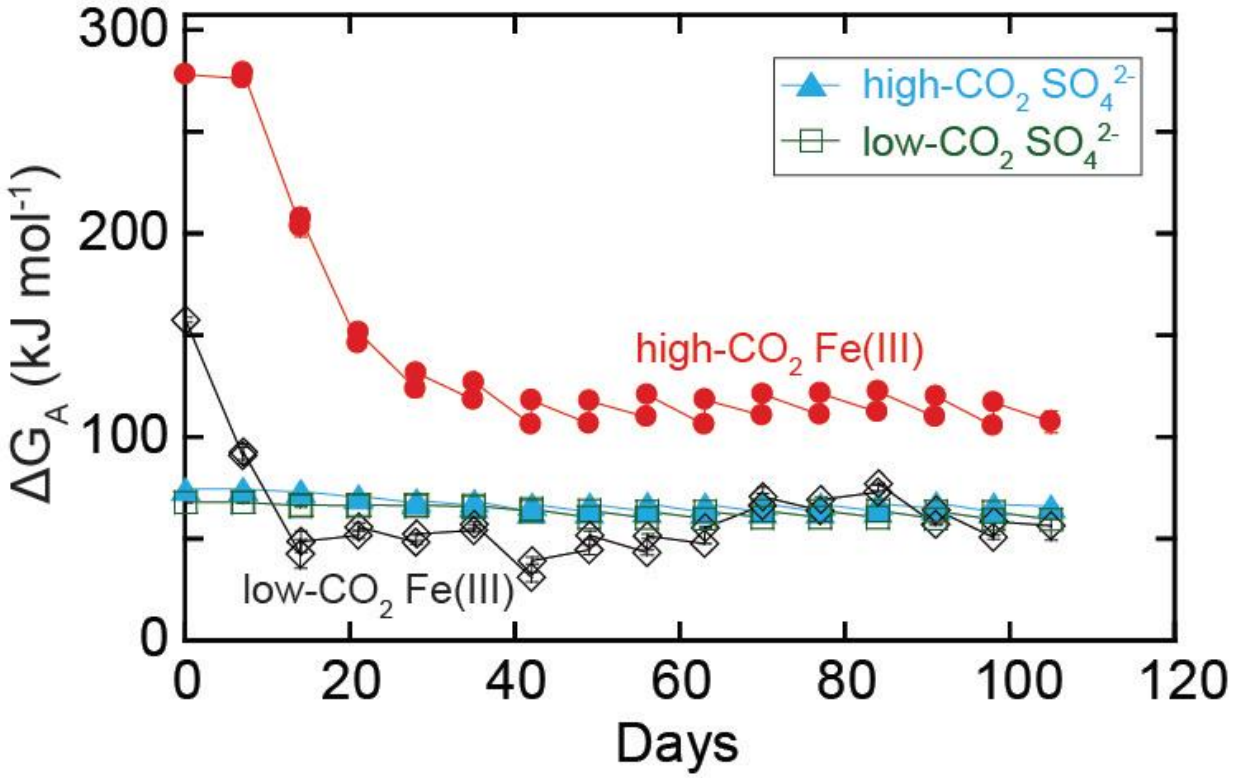

Figure 4. Energy available (ΔG_A) for acetate oxidation coupled to Fe(III) and SO_4^{2-} reduction in the high and low-CO_2 reactors at the beginning and end of each week. Each data point shows the median value calculated for duplicate reactors. The error bars show the range in values for those duplicates.

Figure 5

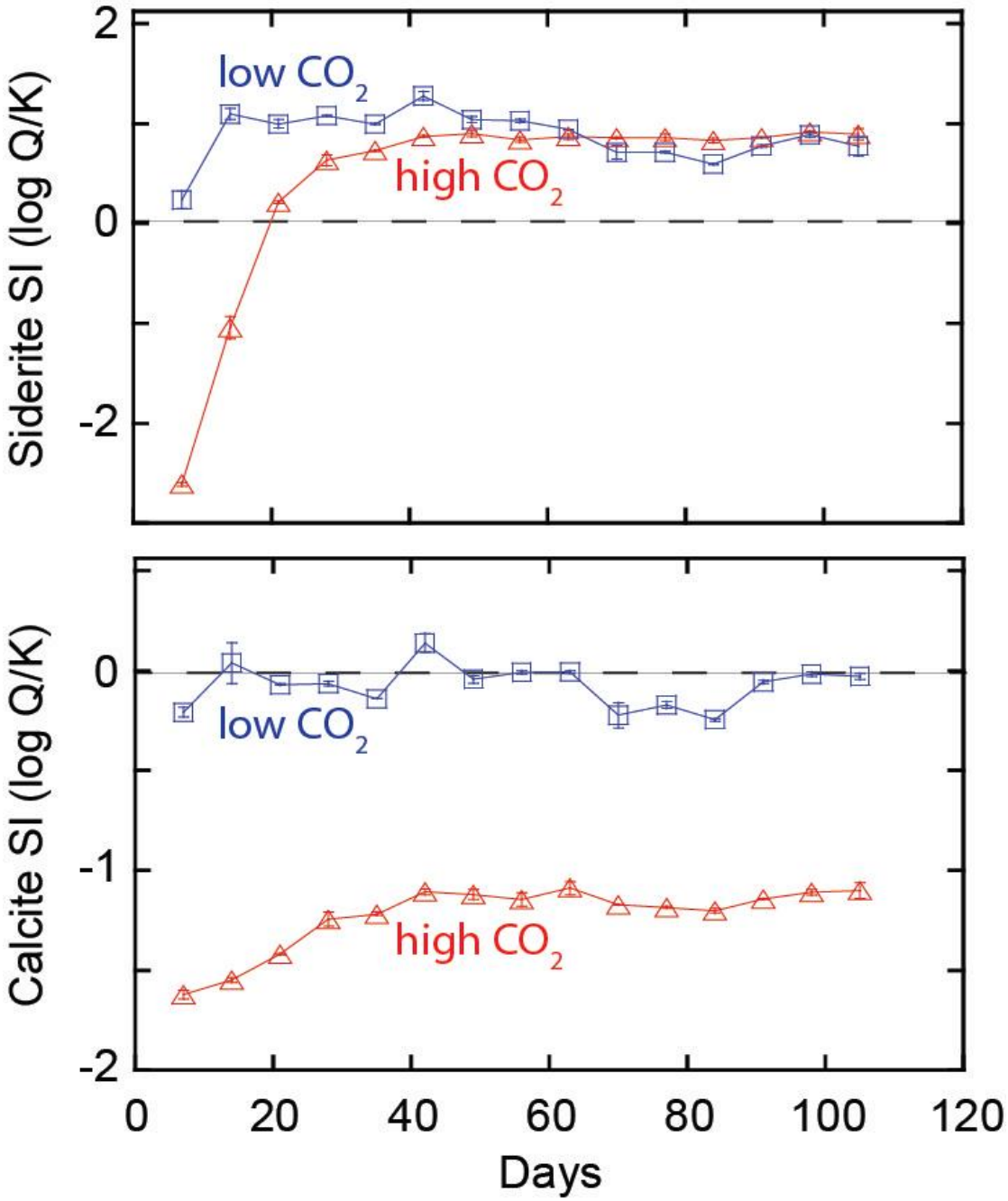

Figure 5. Variation in the saturation index (SI) of siderite ($FeCO_3$) and calcite ($CaCO_3$) in the biologically-active high- and low-CO_2 reactors based on chemical analysis of effluent. Each data point shows the median value calculated for duplicate reactors. The error bars show the range in values for those duplicates. Precipitation of a mineral is thermodynamically favorable where log (Q/K) values are >0.

704 **Figure 6**

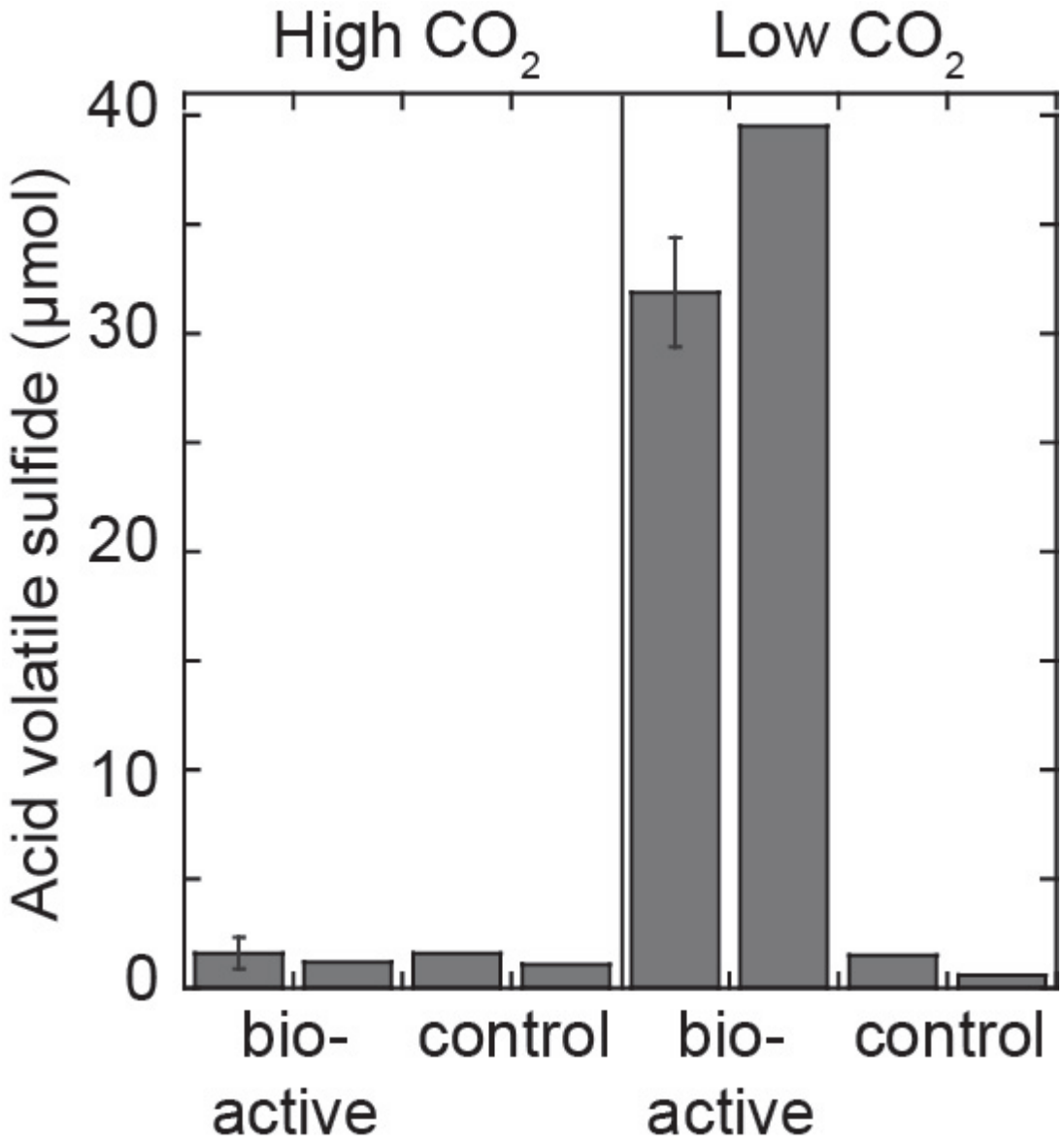

705

706 Figure 6. Acid volatile sulfide (AVS) content of each reactor at the end of the experiment. Results are shown
707 individually for each duplicate reactor. Mean values and error bars corresponding to standard deviation are
708 provided for extractions performed in triplicate (one high-CO_2 and one low-CO_2 reactor).